

MODELING AND SIMULATION OF CNTFET FOR PROSTATE CANCER DETECTION

¹B.N. SHOBHA, ²N.J.R. MUNIRAJ

¹Research Scholar, Department of ECE, Karpagam University, Coimbatore

²Principal, Tejaa Shakthi Institute of Technology for Women, Coimbatore

E-mail: b_n_shobha67@yahoo.com, njrmuniraj@yahoo.com

ABSTRACT

Prostate cancer is the major cancer affecting men and is growing at a very significant rate. One of the major challenges in treatment of prostate cancer is its detection in early stages. The use of Prostate Specific Antigen (PSA) testing has aided the prediction of prostate cancer. It is important to develop an ultrasensitive and selective biological sensor for PSA detection. An ultrasensitive biological detection system that allows the early detection of prostate cancer is expected to improve preventative healthcare. The most widespread techniques for detecting prostate cancer are based on the enzyme-linked immunosorbent assay (ELISA). Recently, biomolecule sensors based on quasi one-dimensional semiconductor nanostructures like nanotubes, nanowires and nanobelts have attracted considerable attention because of their distinct electrical, optical and magnetic properties. Hence, this paper analyzes the device properties of Carbon Nano Tubes (CNT) such as mechanical properties, optical and electrical properties and its relevance as prostate cancer detector or PSA detector. The comparison of MOSFET inverter with CNTFET is also carried out and found that CNTFET has same performance as that of MOSFET with less complexity.

Keywords: *Prostate Specific Antigen, CNTFET Biosensor, CNFET Inverter, CNT-pFET, Low Power Devices*

1. INTRODUCTION

PSA is the enzyme present in the blood stream which is produced in the ducts of the prostate. If the PSA concentration level in the serum is in the range 0 to 4ng/ml, the patient is considered as normal. PSA is used as a biomarker that can detect prostate cancer. However, non cancer diseases such as benign prostatic hyperplasia (BPH), can also result in increased release of PSA into the circulation in blood stream [1]. The use of PSA testing has aided the prediction of prostate cancer risk and treatment outcome. It is important to develop an ultrasensitive and selective biological sensor for PSA detection. An ultrasensitive biological detection system that allows the early detection of prostate cancer is expected to improve preventative healthcare. The most widespread techniques for detecting prostate cancer are based on the enzyme-linked immunosorbent assay [2][3]. Recently, biomolecule sensors based on quasi one-dimensional semiconductor nanostructures, such as nanotubes, nanowires and nanobelts, have attracted considerable attention because of their distinct

electrical, optical and magnetic properties [4][5][6]. The large surface-to-volume ratios and high selective binding of charged biomolecule onto these nanostructure surfaces can result in significant changes of electronic conductance in the channel of the nanostructure [7][8]. In this paper, we analyze the device properties of Carbon Nanotubes such as mechanical properties, optical and electrical properties and its relevance as prostate cancer detector or PSA detector. The development of ultrasensitive FET (Field-effect Transistor) biosensor that is affordable to distinguish between different isoforms of PSA, such as the ratio of free PSA to bound PSA, is inevitable for future disease diagnosis [15]. We also analyze the CNTs for use of transistors and compare their performances with MOSFET.

Section II discusses synthesis of biosensors of cancer detection, section III discusses synthesis of CNT and section IV discusses the use of CNTFET for PSA detection, section V gives comparison of MOSFET inverter with CNFET inverter and conclusion is presented in Section VI.

2. BIOSENSORS FOR PROSTATE CANCER

Figure 1 shows the basic biosensor model. The sensor consists of a bio-receptor that reacts to the presence of a cell/molecule/virus present in an analyte. Bio-receptor triggers the transducer that converts the biological changes to electrical signal that can be detected [9].



Figure 1: Transducers Used in Biosensor Development [9]

Biosensor model need to distinguish between the analyte under investigation and similar molecule, with quick response time. The sensor model should be very selective and specificity for real time measurements. The sensor should be designed to be cost effective, reliable and interoperable over single platform. The data provided by the sensor should be continuous with any changes in analyte concentration and should be reusable. Several nano-devices have been used as biosensors. In the next section we discuss the most prominent nano-bio sensors that have been used for cancer detection.

3. CARBON NANOTUBES

Carbon nanotubes field-effect transistors are recognized as a major topic in nanoelectronics because they can replace traditional MOSFETs in future generations of integrated circuits. In this section the roadmap of CNTFET, its advantages and limitations, fabrication process and challenges in bulk production of CNTFETs, EDA support and libraries are discussed.

As of today, transistors are silicon and germanium substrate based which are expected reach saturation with respect to their channel lengths by the year 2020. As a replacement to this, carbon nanotube based FETs with device performance metrics significantly above those of silicon based MOSFETs are widely reported and studied. CNTFET technology is still in its nascent stage: with device structures still primitive and device physics relatively unexplored. Carbon nanotubes (CNTs) are molecular-scale tubes of graphitic carbon with outstanding properties. CNTs are stronger than steel, harder than diamonds and also possess unique electrical characteristics such as the following: high electrical conductivity, very

high tensile strength, highly flexible, high thermal conductivity and good field emission of electrons [14]. Main advantages of CNTFETs are better control over channel formation, threshold voltage and higher mobility, current density and transconductance. The p-type CNTFET produces three times more on-current per unit width at a gate overdrive of 0.6V compared to a p-type MOSFET at the same gate voltage. Limitations include that the CNTs degrade quickly when exposed to ambient air. Therefore, research is underway to coat CNT with polymers in order to increase their lifetime [10].

3.1 Fabrication Process and Challenges in Bulk Production of CNTFET

CNTFETs are fabricated using techniques such as arc discharge method, chemical vapour deposition, laser ablation to name a few. Carbon nanotubes have many properties, from their unique dimensions to an unusual current conduction mechanism that make them ideal components of electrical circuits. Currently, there is no reliable way to arrange carbon nanotubes into a circuit. The major hurdles that must be jumped for carbon nanotubes to find prominent places in circuits relate to fabrication difficulties. The production of electrical circuits with CNTs is very different from the traditional IC fabrication process. The IC fabrication process is somewhat like sculpture-films are deposited onto a wafer and pattern etched away. Because carbon nanotubes are fundamentally different from films, carbon nanotube circuits so far could not be mass produced [16].

Researchers sometimes resort to manipulating nanotubes one-by-one with the tip of an atomic force microscope in a painstaking, time-consuming process. The best solution is that CNTs can be grown through a chemical vapor deposition process from patterned catalyst material on a wafer, which serve as growth sites and allow designers to position one end of the nanotube. During the deposition process, an electric field can be applied to direct the growth of the nanotubes, which tend to grow along the field lines from negative to positive polarity.

Another way for the self assembly of the CNT transistors consist in using chemical or biological techniques to place the nanotubes from solution to determinate place on a substrate [17]. Even if nanotubes are precisely positioned, the type of nanotubes such as metallic, semiconducting, single-walled, multi-walled cannot be controlled. Figure 2 shows the fabrication steps of CNT.

3.2 CNT Fabrication Steps

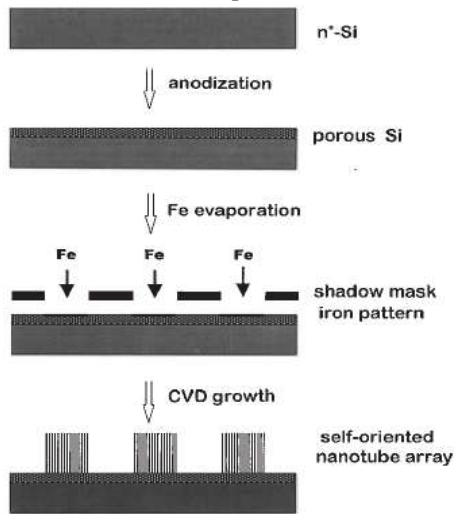


Figure 2: Schematic Process Flow for the Synthesis Of Regular Arrays of Oriented Nanotubes on Porous Silicon by Catalyst Patterning and CVD [11]

Porous silicon samples were obtained by electrochemical etching of P-doped n1-type Si wafers as shown in figure 2. The etching solution contained one part hydrogen fluoride (50% aqueous solution) and one part ethanol and the anodization current density was kept constant at 10 mA/cm². The resulting porous silicon has a thin nanoporous layer on top of a macroporous layer.

The substrates were then annealed which oxidizes the surface of the silicon and the iron. The substrate is placed in a cylindrical quartz boat sealed at one end and then inserted into the center of a 2-inch quartz tube reactor housed in a tube furnace. The furnace is heated to 700°C in flowing Ar. Ethylene was then flown at 1000 sccm for 15 to 60 min, after which the furnace was cooled to room temperature [11].

A chemical engineering solution is needed if nanotubes are to become feasible for commercial circuits. Several process-related challenges need to be addressed before CNT-based devices and interconnects can enter mainstream VLSI manufacturing. Remaining problems include purification, separation, control of length, chirality and the desired alignment, lowering of thermal budget and of high contact resistance. Innovative ideas have been proposed to build practical transistors out of nano-networks. Since lack of control on chirality produces a mix of metallic as well as semi-conducting CNTs from any fabrication process and it is difficult to control the growth direction of the CNTs. Easily-produced random arrays of SWCNTs have been proposed to build

thin film transistors. This idea can be further exploited to build practical CNT based transistors and circuits without the need for precise growth and assembly [12].

3.3 EDA Support and Libraries for CNTFET Based Designs

Resources such as the nanoHUB on the internet which is funded by the National Science Foundation (NSF), act as a gateway for all information related to nano technology. It consists of over 235 simulation tools for nanoelectronics, nanophotonics, etc. Some of the prominent ones include SCHRED, Quantum dot lab, Bulk Monte Carlo tool, Crystal viewer, Band structure lab and Ninithi to name a few. Others such as Ascalaph designer, CoNTub, Nanorex, NEMO 3-D, TubeASP, Tubegen are some of the tools used for modeling of nano structures. Tools such as Hspice from Synopsys allow modeling of CNTFET by using model files, for example by using CNT model files available from the Stanford University Nanoelectronics Group. Ninithi can be used to visualize the 3D molecular geometries of graphene/nano-ribbons, carbon nanotubes (both single wall and multi-wall) and fullerenes. Ninithi also provides features to simulate the electronic band structures of graphene and carbon nanotubes. The graphene structure is shown in figure 3. Ninithi is open source software for research in the field of nanotechnology. This tool is developed by Lanka Software Foundation with assistance from Sri Lanka Institute of Nanotechnology. The tool is helpful to visualize and analyze carbon allotropes in nanotechnology namely Graphene, Carbon nanoribbons, Carbon nanotubes (including multiwall carbon nanotubes) and Fullerenes in 3-D view of the molecular structures [18].

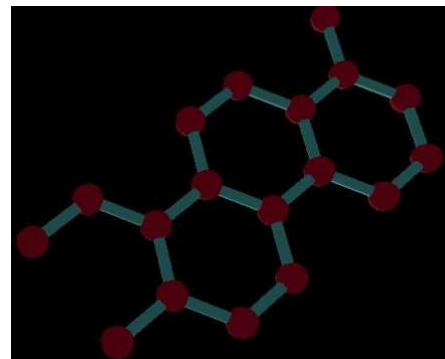


Figure 3: Graphene Structure [18]

It is also possible to visualize the electrical properties of graphene and carbon nanotubes using Ninithi. Entering the properties of inputs M, N and length in angstroms in the settings tab, CNT can be modeled. An example with length of 5 Å with M=3 and N=3 provides the structure as shown in figure 3, length of 6 Å with M=5 and N=5 provides the structure as shown in figure 4.



Figure 4: Carbon Nanoribbon Structure [18]

A carbon nanotube is carbon nanoribbon rolled around an axis perpendicular to the resultant chiral vector. Figure 5 and figure 6 shows the single walled and multiwall CNT rolled using carbon nanoribbon. The electrical properties are obtained by checking the ‘Show electrical properties’ checkbox.

Electrical properties of nanotubes are obtained using the Ninithi tool. The bonding and anti-bonding energy levels can be obtained as shown in figure 7. The electrons within the nuclei of two atoms are placed into the bonding orbitals and electrons which are mostly outside the nuclei of two atoms are placed into anti-bonding orbitals.

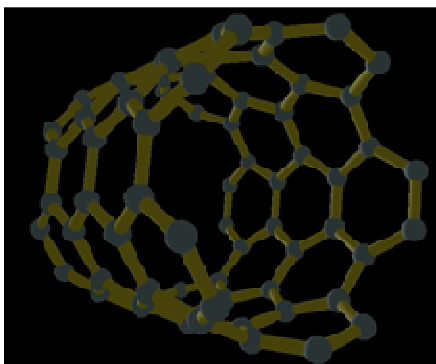


Figure 5: Carbon Nanotube Structure [18]

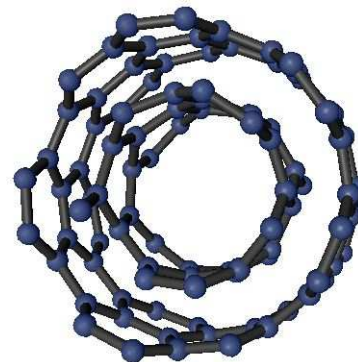


Figure 6: Multi Wall Carbon Nanotube [18]

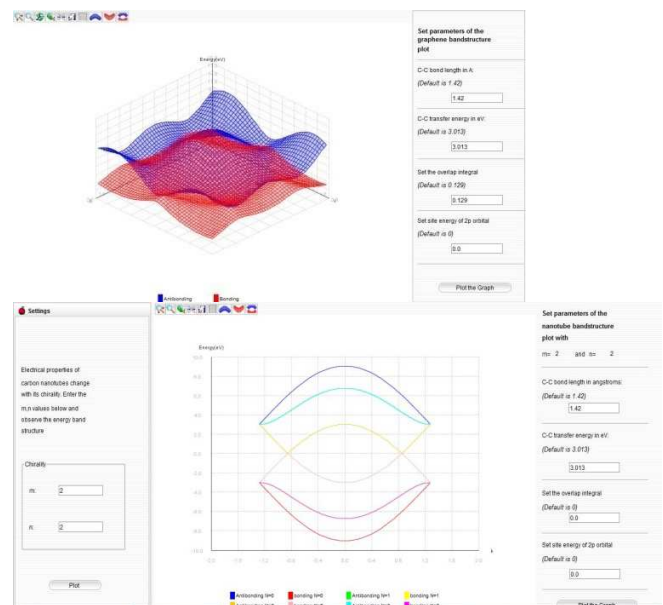


Figure 7: Electrical Properties of Graphene and Carbon Nanotube

The data of the plot is also available in tabular form by using the graph data. The C-C bond length, C-C transfer energy in eV (electron volt), overlap integral and site energy of 2p orbital needs to be entered by the user and the graph can be plotted. The chiral integers M and N need to be additionally entered for analysis of carbon nanotube. Linear and logarithmic scale settings are allowed.

Many of the EDA companies are working on including CNTs libraries in their tool portfolio. The scalability of CNTFETs, which is a major requirement for replacing MOSFETs in logic applications or for being used in memory technology, needs to be investigated more in detail.

For example, CNTFETs with sub-100 nm channel length could be fabricated by means of electron beam lithography. Rise in demand, production and ease of accessibility of carbon nanotubes would lead to the extensive use of carbon nanotubes in a wide variety of applications. The use of nanotechnology for human will become common need in 21st century.

4. CNTFET TECHNOLOGY [19]

CNTs are sheets of graphene rolled into tubes, depending on the chirality (i.e., the direction in which the graphene sheet is rolled), a single-walled CNT can be either metallic or semiconducting. Semiconducting nanotubes have attracted widespread attention of device/circuit designers as an alternative possible channel implementation for high-performance transistors. A typical structure of a MOSFET-like CNFET device is illustrated in figure 7. The CNT channel region is undoped, while the other regions are heavily doped, thus acting as the source/drain extended region and/or interconnects between two adjacent devices. Carbon nanotubes are high-aspect-ratio cylinders of carbon atoms.

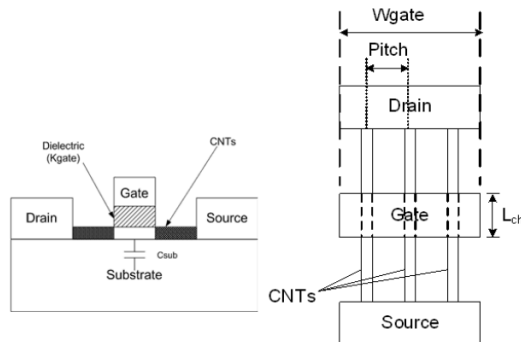


Figure 8: CNTFET Structure [19]

The electrical properties of a single wall carbon nanotube offer the potential for molecular-scale electronics, a typical semiconducting single-wall carbon nanotube is 1.4nm in diameter with a 0.6eV band-gap (the band-gap is inversely proportional to the diameter). Recent Carbon Nanotube Field Effect Transistors (CNFETs) have a metal carbide source/drain contact and a top gated structure as in figure 8 with thin gate dielectrics.

The contact resistance and the subthreshold slope of a CNTFET are comparable to those of silicon MOSFET. While a silicon FET's current drive is typically measured in current per unit device width (e.g. $\mu A = \mu m$), the CNFET's current is

measured in current per tube (as reflecting the structure of the CNFET as an array of equal carbon nanotubes with constant spacing and fixed diameter).

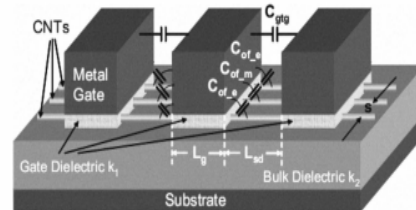


Figure 9: 3-D Structure of CNTFET [13]

Figure 9 shows a 3-D device structure of CNTFET with multiple channels, high K (dielectric constant) metal gate and parasitic gate capacitances. There are three transistors fabricated along one carbon nanotube. A circuit-compatible compact model is used for the intrinsic channel region of the MOSFET like CNTFETs. This model can be used for wide range of diameters and other structural variables. In the model itself, the global device parameters of the transistor have been kept constant and were suggested not to be altered. There are two different models for CNTFET from SUNG: Standard model and Uniform model. Both the models allow multiple carbon nanotube under the same gate, the only difference being the way it treats the charge screening effects. In the standard model the charge screening effects between the multiple nanotubes in the same device are modeled, where as in uniform model the charge screening effects are considered uniform.

In this work we use the standard model, as it is the more accurate and faster when compared to the uniform model. The precision of the Stanford model can be explained by the several non-idealities assimilated such as scattering, effects of the doped source/drain extension region, Schottky barrier resistance and inter-CNT charge screening effects. The quasi-ID device structure gives better gate electrostatics control over the gate region. Increasing the number of CNTs per device is the most effective way to improve the on current. The model utilizes a semiconducting nanotube, with a chirality vector (19, 0). The effective length of the wire is 32nm.

4.1 CNTFET Properties

To measure the actual performance of a CNTFET and for properties, CNTFET should be understood by the I-V characteristics. It is

important to know the characteristics of a single CNT based transistor. In this section, the basic characteristics in terms of the current and voltage across a single transistor is done by using Stanford 32 nm model-file in H-Spice simulator.

Table 1: Device Parameters and Process Assumptions for Simulations (CNTFET Model) [13]

| Variable Parameters | |
|--|--|
| Source/Drain Doping Level | 0.59 eV - 0.75 eV (0.7% - 1.3%) Uniformly distributed* |
| CNT Diameter | 1.2 nm - 1.8 nm Uniformly distributed* |
| Probability of a CNT to be Metallic | 8% - 32% |
| Fixed Parameters | |
| Oxide Thickness (T_{ox}) | 4 nm |
| Gate Dielectric (Dielectric Constant: K_{ox}) | HfO ₂ (16) |
| CNT Pitch | 4 nm |
| Power Supply | 0.9V |
| Mean Free Path: Intrinsic CNT | 200 nm |
| Mean Free Path: Doped CNT | 15 nm |
| Gate/Source/Drain Length (CNT) | 32 nm |
| Work Function: contact (Φ_{M1}) | 4.5 eV |
| Work Function: CNT (Φ_{CNT}) | 4.5 eV |
| Interconnect Capacitance | 0.22 fF/ μ m |

The basic characteristics are delay, power, PDP, leakage current and frequency response are simulated and compared. In CNTFET also two types of transistors are available one is NFET & second one is PFET.

- Used model-file for MOSFET: PTM Low Power 32nm Metal Gate/High-K/Strained-Si
- Used model-file for CNTFET: Stanford library, HSPICE Models Version 2.2.1.

Number of CNT tubes is 3, chirality single dimension (19, 0) and effective length is 32 nm.

4.2 Input Characteristics

The input characteristics curve is drawn between the input voltage V_{gs} and the output drain current. The simulation result for both CNTFET's with 32 nm MOSFET is shown in figures 10 & 11.

Figures 10 and 11 show the input characteristics of nFET and pFET with MOSFETs. In general, CNTFET has higher ON current compared to MOSFET for the same OFF current. Due to the small molecular structure of the CNTFET device, scaling the future size, beyond what currently available advanced lithographic methods permit, is possible. The great advantage of CNTFET device is that its threshold voltage can be determined just by

adopting a proper diameter for its CNTs. This practical attribute makes CNTFET more flexible than MOSFET for designing digital circuits and makes it very suitable for designing multi-Vth circuits. The threshold voltage of a CNTFET is approximately considered as the half band-gap. The nFET V_{th} is 0.25 V and for pFET is -27 V shown in figures 10 and 11.

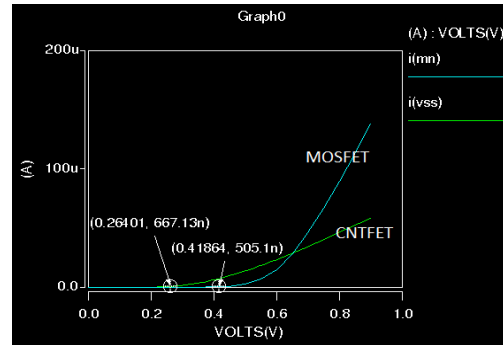


Figure 10: CNT-nFET and NMOS Input Characteristics

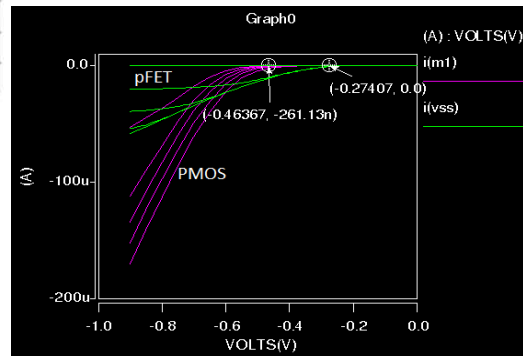


Figure 11: CNT-pFET and PMOS Input Characteristics

The ON current is increasing linearly with the input voltage V_{gs} . The CNT will provide the high channel mobility so automatically current will increase and linearity is more. The current is drastically increasing in CNTFET with increasing of number of tubes.

4.3 Output Characteristics

The output characteristic curve is drawn between the drain to source voltage (V_{ds}) and drain current (I_{drain}) for the constant different source to gate voltages (V_{gs}). This characteristic curve gives the pinch-off, linearity and the effect of drain resistance. Figure 12 and figure 13 shows the output characteristics of CNTFET and 32nm MOSFET transistors.

The output characteristic shows that the saturation current in CNTFET is more stable than 32 nm MOSFET. The CNTFET is used as a best current source with accuracy in small scale technology. The effect of drain resistance is less in CNTFET as the current becomes constant, whereas the effect of drain resistance is high in MOSFET and the current is not constant

the square wave is 33.33 MHz. For a supply of 1.8 V, the response as shown in figure 14 is obtained. The frequency is gradually increased and the maximum operating frequency of the inverter is obtained at 10 GHz. The maximum output current is obtained by varying VDD and obtained as 183.04 μ A. This corresponds to the region of operation of the inverter where both PMOS and NMOS transistor are ON.

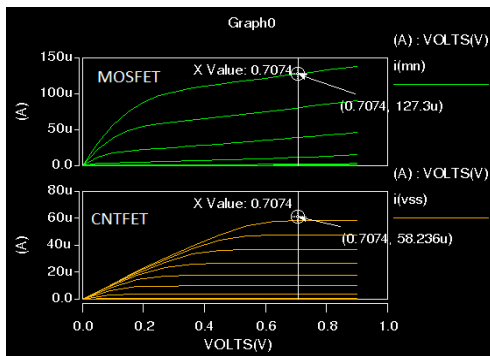


Figure 12: CNT-nFET and NMOS Output Characteristics

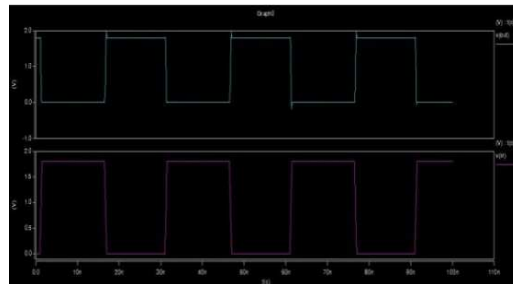


Figure 14: Inverter Output using MOSFET

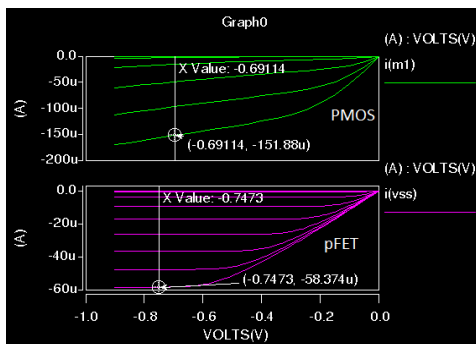


Figure 13: CNT-pFET and PMOS Input Characteristics

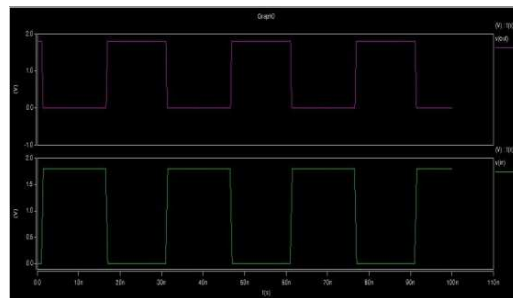


Figure 15: Inverter output using CNFET

The current of the CNTFET can be increased by increasing the number of tubes in a CNTFET at room temperature. The leakage power is also reduced due to the high stability in saturation current and due to back gate control saturation current decreased with high performance. The drain current with 3 tubes is 58.236 μ A in nFET and 58.37 μ A in pFET at $V_{ds}=7.024V$.

The frequency of the square wave is 33.33 MHz for the CNFET inverter. For a supply of 1.8 V the response as shown in figure 15 is obtained. The frequency is gradually increased and the maximum operating frequency of the inverter is obtained beyond 10 GHz. The response is the same as that obtained using the MOSFET but with less glitches. For 10 GHz the response of the CNFET inverter is better than that of MOSFET. The maximum output current is obtained by varying VDD and obtained as 58.396 μ A. The static voltage transfer characteristic of CMOS based inverter is shown in figure 16.

5. COMPARISON OF MOSFET INVERTER WITH CNFET INVERTER

The MOSFET inverter analysis is carried out by providing a pulse input. Initially the frequency of

Similar response is obtained by CNFET based inverter as shown in figure 17. The noise margins in both cases are very similar V_{IL} is around 0.6 V and V_{IH} is 1.15 V. For all designs discussed so far, the integers $M=19$, $N=0$ for the CNTFET

considered indicating zigzag carbon nanotube structure.

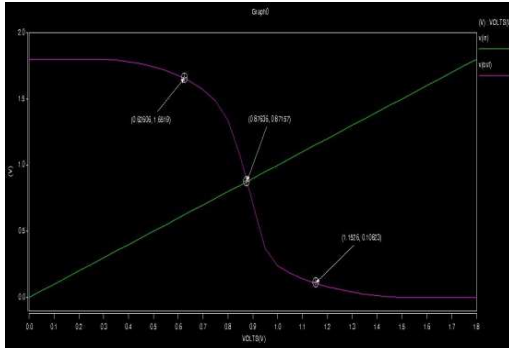


Figure 16: VTC of CMOS Inverter

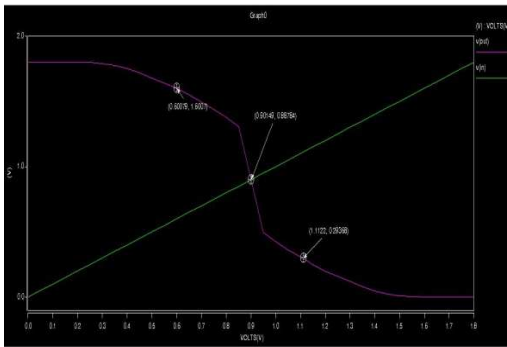


Figure 17: VTC of CNTFET Inverter

Surface Immobilization of CNTFET Biosensors

CNTFET consisting of source drain regions being connected with CNT as the channel is cleaned in acetone and ethanol mixing solution. By self-assembling process monolayers are formed on the surface of channel by engrossing sample into a solution of 10 % APTES aqueous for 30 min, washed with DI water and heated at 120°C for 30 min. The device is rinsed with glutaraldehyde in phosphate buffered saline. Further, the CNTFET device is immersed in prostate specific antibody (anti-PSA) solution for more than 12 hours at 4°C. With this process anti-PSA is linked to the aldehyde groups to form a CNTFET biosensor. After the attachment of anti-PSA molecule, the prostate cancer marker PSA is reacted to bind with the anti-PSA molecule from the CNTFET sensor surface [15]. The PSA marker present in the solution reacts with the anti-PSA molecule on the CNTFET channel to change the gate voltage, thus controlling the current to flow through the channel measured at the drain end. Higher concentration of

PSA agent in the solution increases the drain current and hence CNTFET sensor readings are calibrated for detecting prostate cancer.

A label-free CNTFET biosensor that allows efficient PSA biosensing is proposed and demonstrated in [15]. The CNTFET device is fabricated and operated under n-channel depletion characteristics. The aldehyde groups from the glutaraldehyde linked to the amino groups of APTES is attached on the biosensor surface to immobilize anti-PSA molecules. The output signal of the developed CNTFET biosensor can be used to detect PSA concentration in the range from 5 to 5000 pg/mL. To improve the sensing sensitivity of PSA molecule, this biosensor can be improved by inserting arginine molecule between glutaraldehyde and APTES [15]. A real-time detection of breast cancer cells through label-free protein biosensors based on antibody-conjugated CNTFETs has been demonstrated [20].

6. CONCLUSION

There is very less information in literature about comparison of CNTFET and MOSFET for detection of prostate cancer. The conclusion from this comparative analysis is that CNTFET have same performance as that of MOSFET. The inverter being the basic circuit in building larger logic designs it is clear from this experiment that the Carbon nanotube FET can replace MOSFETs in complex designs as well as they provide the same performance. The characteristics of CNTFET prove that they can be used as sensors in biomedical applications; also the signal conditioning unit can be realized using CNTFET.

The current handling capability demonstrate their advantages as low power devices and suitable for portable applications. Because this label-free CNTFET biosensor demonstrates the ability to detect the lower concentration of PSA molecule, such biosensor has demonstrated the potentially useful platform for biological research, prostate cancer screening and palliative care for prostate cancer patients in the future.

The authors acknowledge the support and guidance provided by Dr. Cyril Prasanna Raj P. His inputs and timely guidance has helped us to carry out the experimental analysis.

REFERENCES:

- [1] Ulf-Håkan Stenman, Jari Leinonen, Wan-Ming Zhang and Patrik Finne, "Prostate-specific Antigen", *Seminars in Cancer Biology*, Vol. 9, issue 2, April 1999, pp. 83-93
- [2] K. L. Moore, A. F. Dalley, A. M. R. Agur, P. W. Tank and T. R. Gest, "Clinically Oriented Anatomy", 6th edition, 2009
- [3] Xiaowu Tang, Sarunya Bansaruntip, Nozomi Nakayama, Erhan Yenilmez, Ying-lan Chang and Qian Wang, "Carbon Nanotube DNA Sensor and Sensing Mechanism", *Nano Letters*, Vol. 6, No. 8, 2006, pp. 1632-1636
- [4] Fernando Patolsky, Gengfeng Zheng and Charles M Lieber, "Fabrication of Silicon Nanowire Devices for Ultrasensitive, Label-free, Real-time Detection of Biological and Chemical Species", *Nature Protocols*, Vol 1, 2006, pp. 1711-1724
- [5] Y. Cheng, P. Xiong, C. S. Yun, G. F. Strouse, J. P. Zheng, R. S. Yang and Z. L. Wang, "Mechanism and Optimization of pH Sensing using SNO₂ Nanobelt FETs", *Nano Letters*, 8(2008), pp. 4179-4184
- [6] Min Zhang, Faliang Cheng, Zhiquan Cai and Haijun Yao, "Glucose Biosensor Based on Highly Dispersed Au Nanoparticles Supported on Palladium Nanowire Arrays", *International Journal of Electrochemical Science*, Vol 5 (2010), pp. 1026-1031
- [7] Chih-Heng Lin, Cheng-Yun Hsiao, Cheng-Hsiung Hung, Yen-Ren Lo, Cheng-Che Lee, Chung-Jung Su, Horng-Chin Lin, Fu-Hsiang Ko, Tiao-Yuan Huang and Yuh-Shyong Yang, "Ultra-Sensitive Detection of Dopamine Using Polysilicon Nanowire FET", *Chem. Commn*, 2008, pp. 5749-5751
- [8] Cheng-Yun Hsiao, Chih-Heng Lin, Cheng-Hsiung Hung, Chun-Jung Su, Yen-Ren Lo, Cheng-Che Lee, Horng-Chin Lin, Fu-Hsiang Ko, Tiao-Yuan Huang, Yuh-Shyong Yang, "Novel Poly-silicon Nanowire Field Effect Transistor for Biosensing Application", *Biosensors and Bioelectronics*, Vol 24, issue 5, 2009, pp. 1223-1229
- [9] Anil Deisingh, "Biosensors for Microbial Detection", *Microbiologist*, June 2003, pp. 30-33
- [10] Latisha Crockett, "Carbon Nanotube Transistor Fabrication and Reliability Characterization", *REU Research Accomplishments*, 2009, pp. 46-47
- [11] Shoushan Fan, Michael G. Chapline, Nathan R. Franklin, Thomas W. Tomblor, Alan M. Cassell and Hongjie Dai "Self-Oriented Regular Arrays of Carbon Nanotubes and Their Field Emission Properties", *Science* 283, 1999, pp. 512-514
- [12] Sergey Yatsunenkov, Witold Lojkowski, Goran Markovic and Jonathan Loeffler, "A Technology Roadmap for SMEs on New Photonic Devices, Materials and Fabrication Technologies", *Photonics in Safety and Security*, September 2009
- [13] Jie Deng, H. S. Philip Wong, "Including Non-idealities and its Application-Part I: Model of the intrinsic Channel region and Part 2: Full device model and circuit performance benchmarking", *IEEE Transaction on Electron Devices*, Vol.54, No A Compact SPICE Model for Carbon Nanotube Field Effect Transistors 12, December 2007
- [14] Anuj Pushkama, Sajna Raghavan and Hamid Mahmoodi, "Comparison of Performance Parameters of SRAM Designs in 160m CMOS AND CNTFET Technologies", *School of Engineering, San Francisco State University, San Francisco, CA, USA*
- [15] Chi-Chang Wu, Tung-Ming Pan, Chung-Shu Wu, Li-Chen Yen, Cheng-Keng Chuang, See-Tong Pang, Yuh-Shyong Yang and Fu-Hsiang Ko, "Label-free Detection of Prostate Specific Antigen Using a Silicon Nanobelt Field-effect Transistor" *International Journal of Electrochemicals Science*, Vol 7, pp. 4432-4442, 2012
- [16] <http://www.slideshare.net/neerajparmar68/composites-11956937>
- [17] K.S. Swapna, "Nano Carbon Tubes: an Application of Nano-technology", *Carbon*, vol. 33
- [18] <http://niniti.software.informer.com>
- [19] Young Bok Kim, Yong-Bin Kim and Fabrizio Lombardi. "A Novel Design Methodology to Optimize the Speed and Power of the CNTFET Circuits", *52nd IEEE International Midwest Symposium on Circuits and Systems, MWSCAS*, 2009
- [20] Teker, Kasif, "Bioconjugated carbon nanotubes for targeting cancer biomarkers", *Solid-State Materials for Advanced Technology*; v.153, pp. 1-3